Pol. J. Environ. Stud. Vol. XX, No. X (XXXX), 1-13
DOI: *10.15244/pjoes/216154* ONLINE PUBLICATION DATE: 2026-02-26

Original Research

Oxidative Degradation of Aniline by Ferrate-Hydrogen Peroxide System: Unveiling pH-Dependent Mechanisms and Pathways

Feihu Zeng[1○]*, Zhiwen Wang[1], Ruolan Lin[1], Syyi Sim[2], Feng Wang[1], Xianfeng Huang[3]

[1]Liming Vocational University, Quanzhou, 362000, China
[2]Faculty of Electrical and Electronic Engineering, Universiti Tun Hussein Onn Malaysia, Johor, Malaysia
[3]School of Life and Environmental Science, Wenzhou University, Wenzhou, 325035, China

Received: 07 September 2025
Accepted: 28 December 2025

Abstract

This study systematically investigated the efficacy and underlying mechanisms of aniline degradation in a Ferrate (Fe(VI))-hydrogen peroxide (H_2O_2) system. The effects of key operational parameters, including H_2O_2 dosage, initial pH (3-11), and reaction temperature (10-60ºC), were evaluated. Under optimal conditions (10 mM Fe(VI), 176 mM H_2O_2, 30ºC, 30 min), high aniline removal efficiencies of 91±0.3% and 88±0.2% were achieved at pH 3.0 and 7.0, respectively. Radical quenching experiments with tert-butanol, coupled with kinetic modeling, revealed a critical pH-dependent mechanistic shift. Under acidic conditions (pH 3.0), the degradation followed pseudo-second-order kinetics (k_{app} = 0.03425 $mM^{-1}\cdot min^{-1}$), with hydroxyl radicals (·OH) identified as a primary oxidizing species. In contrast, under alkaline conditions, the process was dominated by high-valent iron species (Fe(IV)/Fe(V)) and direct electron transfer by Fe(VI), adhering to pseudo-first-order kinetics (maximum k_{app} = 0.07319 min^{-1}). Fourteen intermediate products were identified via liquid chromatography–mass spectrometry (LC–MS), leading to the proposal of four potential degradation pathways. This work provides fundamental insights into the pH-dependent mechanisms of the Fe(VI)/H_2O_2 system and proposes a promising, sustainable strategy for the treatment of aniline-containing industrial wastewater.

Keywords: ferrate, hydrogen peroxide, aniline, mechanism, reaction pathways

*e-mail: 20132729@lmu.edu.cn
Tel.: +86-13859765695
Fax: +86-0595-22900160
°ORCID iD: 0009-0002-7144-9908

Introduction

Aniline (C_6H_7N), an important chemical intermediate, is widely used in the defense, dyeing, and pharmaceutical industries. However, aniline-containing wastewater is not only recalcitrant to biodegradation but also highly toxic to aquatic life. It has been classified as a Group 2B carcinogen by the International Agency for Research on Cancer (IARC), posing serious risks to ecosystems and human health [1]. Existing methods for aniline treatment are often inadequate. Physical adsorption is ineffective as it transfers, rather than degrades, aniline [2]; biological techniques pose challenges in adapting to high aniline concentrations [3]; and conventional advanced oxidation processes (AOPs), including Fenton reactions, though efficient, are hampered by a narrow pH applicability (2-7), iron sludge accumulation, and catalyst deactivation [4-6]. Therefore, it is of great significance to develop efficient, environmentally friendly, and pH-tolerant technologies for aniline degradation.

Ferrate (Fe(VI)), a green strong oxidant (E^0 = 0.7-2.2 V) [7], combines oxidation, disinfection, and coagulation functions, and is reduced to non-toxic Fe(III), demonstrating considerable potential in degrading refractory organic compounds. Studies have shown that Fe(VI) can oxidize aniline via radical pathways, yielding nitrobenzene or polymeric coupling products such as azobenzene [8]. Guo et al. also reported that ·OH generated during Fe(VI) degradation of aniline could further enhance the removal of co-pollutants like tetracycline [9]. In recent years, the synergistic oxidation system comprising Fe(VI) and hydrogen peroxide (H_2O_2) has attracted widespread attention [10]. The introduction of H_2O_2 activates Fe(VI) to form higher-valent iron species (Fe(IV)/Fe(V)) and various radicals (e.g.,·OH and $O_2^{\cdot-}$), thereby significantly enhancing oxidative capacity [11, 12]. The Fe(VI)/H_2O_2 system has been successfully applied in the treatment of various organic wastewaters, demonstrating effective removal of bisphenol A (BPA) [11] and dimethyl phthalate (DMP) [13] from contaminated streams. It has also shown promising results in pharmaceutical wastewater treatment. For instance, Samira et al. [14] reported efficient degradation of sulfamethoxazole under acidic conditions (pH = 3). Shi et al. [15] achieved a chemical oxygen demand (COD) removal efficiency exceeding 95% when treating neomycin sulfate wastewater. The better oxidation performance of the Fe(VI)–H_2O_2 system than Fe(VI) alone was ascribed to the catalytic role of in-situ and ex-situ H_2O_2, which can directly and/or indirectly facilitate the formation of Fe(IV) and Fe(V) [16].

The oxidative performance of the Fe(VI)/H_2O_2 system is critically influenced by solution pH. Under highly acidic conditions, Fe(VI) is susceptible to hydrolysis, whereas under alkaline conditions, its excessive stability occurs; both scenarios consequently diminish the utilization efficiency of H_2O_2 [13]. In aqueous solution, Fe(VI) exists mainly as $HFeO_4^-$ (pH 3.5-7.2) and FeO_4^{2-} (pH>7.2) [17], and the reactivity varies considerably among species, resulting in distinct degradation behaviors for different pollutants under varying pH conditions. Furthermore, the reaction pathways remain controversial; for example, Wen et al. proposed coexisting self-reduction pathways of Fe(V)/Fe(IV) and a Fe(IV) → Fe(III) → $\cdot O_2^-$ pathway in this system [18]. Although the Fe(VI)/H_2O_2 system shows promising application potential for organic pollutant degradation, several critical knowledge gaps remain concerning its application to aniline, a priority toxic pollutant. First, the pH-dependent mechanistic shift between radical and non-radical pathways within this specific system is not well-quantified or conclusively demonstrated for aniline degradation. Second, the relative contribution of active species (e.g., OH, Fe(IV)/Fe(V), Fe(VI) itself) across a wide pH range remains ambiguous and lacks direct experimental validation through methods like controlled quenching studies. Third, a comprehensive degradation pathway for aniline based on identified intermediates, and how this pathway evolves with pH, has not been systematically established for the Fe(VI)/H_2O_2 system.

Therefore, this study aims to fill these gaps by systematically investigating the degradation behavior of aniline by the Fe(VI)/H_2O_2 system over a broad pH range (3-11). We quantitatively elucidate the pH-dependent kinetics, employ radical quenching experiments to delineate the shift in dominant active species, and identify intermediate products via LC-MS to propose conclusive degradation pathways. This work provides fundamental insights necessary for the targeted application of this promising technology.

Materials and Methods

Chemicals and Reagents

All chemical reagents were of analytical grade and used without further purification. Deionized water (resistivity of 18.2 MΩ·cm) was used for the preparation of all aqueous solutions.

Specifically, aniline ($C_6H_5NH_2$, ≥99.5%), potassium ferrate (K_2FeO_4, ≥96%), sodium thiosulfate ($Na_2S_2O_3$, ≥99%), sodium nitrite ($NaNO_2$, ≥99%), and N-(1-Naphthyl)ethylenediamine dihydrochloride ($C_{12}H_{16}Cl_2N_2$, ≥99%) were purchased from Sinopharm Chemical Reagent Co., Ltd. (China). Ammonium sulfamate ($NH_4SO_3NH_2$, ≥99%), sodium hydroxide (NaOH, ≥99%), hydrogen peroxide (H_2O_2, 30% w/v), tert-butanol ($C_4H_{10}O$, ≥99%), hydrochloric acid (HCl, 36% w/v), and sulfuric acid (H_2SO_4, 95% w/w) aqueous solution were procured from Xilong Scientific Co., Ltd. (China).

Aniline Degradation Experiments

The aniline degradation experiments were conducted in a batch mode using a constant-temperature magnetic stirring water bath. Briefly, a prepared aniline stock solution (250 mL, 10 mM aniline) was mixed with oxidants (Fe(VI) and H_2O_2) in the reactor. The solution pH and temperature were maintained at predetermined values using pH stat controllers and the water bath, respectively. At designated time intervals, aliquots were withdrawn from the reaction mixture and immediately quenched by adding sodium thiosulfate to terminate the reaction. The quenched samples were then filtered through 0.22 μm aqueous phase syringe filters, appropriately diluted, and analyzed for residual aniline concentration. All experiments were conducted in triplicate, and the results are presented as mean values±standard deviation.

Radical Quenching Experiments

To identify the contribution of radical species to aniline degradation, quenching experiments were performed by introducing tert-butanol (TBA), a common hydroxyl radical quencher, into the reaction system. The experimental procedure was like that described in aniline degradation experiments, with the following modifications: A predetermined amount of TBA (100 mL) was first mixed with the aniline solution (250 mL, 10 mM), and the pH was adjusted to the target value using dilute HCl and NaOH solutions. Subsequently, the oxidants (10 mM Fe(VI) and 176 mM H_2O_2) were added to initiate the reaction. Sampling, quenching, filtration, and analysis followed the identical protocol outlined above.

Analytical Methods

The concentration of aniline was determined according to the Chinese National Standard method (GB/T 11889-1989) [19] based on azo spectrophotometry. This method involves a diazotization and coupling reaction to form a colored azo compound, the absorbance of which is measured spectrophotometrically at a specific wavelength (typically around 545 nm) for quantification.

Intermediate products generated during aniline degradation were identified using liquid chromatography–mass spectrometry (LC–MS) equipped with a Hypersil Gold column (2.1 mm × 100 mm, 1.9 μm) held at 30ºC. The mass spectrometer was operated in negative MS2 scan mode, scanning from m/z 50 to 500. The mobile phase comprised water (A) and acetonitrile (B), with a flow rate of 0.2 $mL \cdot min^{-1}$. The limit of detection (LOD) and limit of quantification (LOQ) for this method were 0.08 $\mu g \cdot L^{-1}$ and 0.27 $\mu g \cdot L^{-1}$, respectively.

Results and Discussion

Different Oxidizing Agents

To investigate the synergistic effect between Fe(VI) and H_2O_2, the performance of three oxidation systems – 10 mM Fe(VI) alone, 170 mM H_2O_2 alone, and their combination (10 mM Fe(VI) + 170 mM H_2O_2) – was compared under the conditions of T = 30ºC, pH = 6.8, and an initial aniline concentration of 10 mM. The degradation efficiency is presented in Fig. 1.

After 15 min of reaction, the removal rates of aniline by Fe(VI) alone and H_2O_2 alone were 33.67±0.2% and 55.13±0.1%, respectively. Notably, the Fe(VI)-H_2O_2 combined system achieved a degradation efficiency of 86.41±0.5%, which was significantly superior to either system alone, indicating a distinct synergistic effect. However, the efficiency of the combined system was slightly lower than the sum of the individual systems' efficiencies (88.80%). This result contrasts sharply with the supra-additive effect (1+1>2) reported by Fitri et al. [20] for bisphenol A degradation using the same system.

We hypothesize that this discrepancy originates from the specific reaction conditions. Under the near-neutral pH (6.8) condition of this study, aniline ($pK_a \approx 4.6$) exists primarily in its neutral molecular form. More critically, the speciation and stability of Fe(VI) are highly pH dependent. While Fe(VI) exists as the stable FeO_4^{2-} species in alkaline media, favoring its reaction with H_2O_2 to generate highly active species, its chemical behavior is more complex at the pH used here. The massive introduction of *ex-situ* H_2O_2 might inhibit the function of trace *in-situ* H_2O_2 produced from the self-decomposition of Fe(VI), which could play a pivotal role in driving the continuous and efficient generation of reactive intermediates from Fe(VI).

Notwithstanding, the combined system still exhibited a significant synergistic effect, primarily attributable to the interactions between H_2O_2 and Fe(VI). As described by Eqs. (1) to (4):

$$Fe(VI) + H_2O_2 \longrightarrow Fe(V) + HO_2 \cdot + OH^- \quad (1)$$

$$Fe(V) + H_2O_2 \longrightarrow Fe(IV) + \cdot OH + OH^- \quad (2)$$

$$Fe(VI) + H_2O_2 \longrightarrow Fe(IV) + O_2 + H_2O \quad (3)$$

$$Fe(VI) + H_2O_2 \longrightarrow Fe(III) + O_2 + \cdot OH \quad (4)$$

H_2O_2 ($E^0 = 1.77$ V) [21], by virtue of its peroxy bond (O-O), tends to undergo a two-electron transfer process, reducing Fe(VI) and thereby directly or indirectly accelerating the generation of higher-valent iron species (Fe(IV)/Fe(V)). Concurrently, this process also produces strong oxidizing species such as hydroxyl radicals (OH, $E^0 = 2.8$ V [22]), collectively contributing to enhanced aniline degradation. However, the excess H_2O_2 might also act as a scavenger, consuming portions of the newly formed active species (e.g., Fe(IV)/Fe(V) and ·OH),

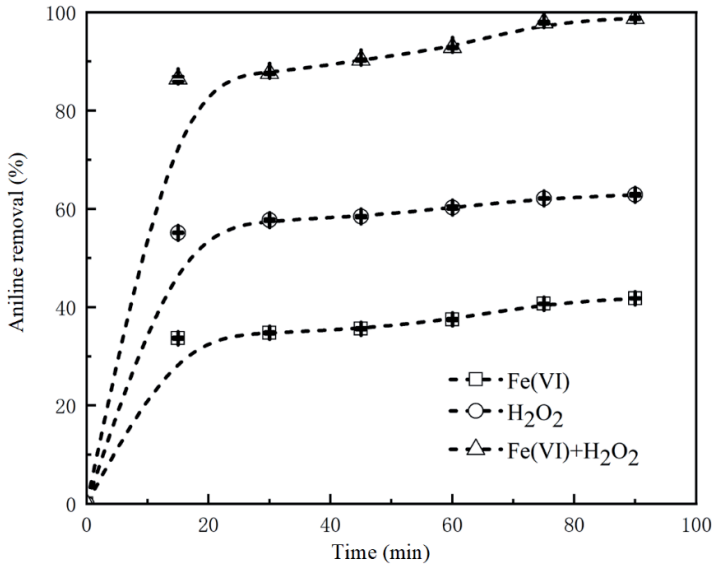

Fig. 1. Influence of different oxidations on the degradation effect of aniline.
(Reaction conditions: T = 30ºC, pH = 6.8, 10 mM aniline, oxidizing agent: 10 mM Fe(VI), 176 mM H_2O_2, and 10 mM Fe(VI) + 176 mM H_2O_2)

which partly explains why the synergistic effect did not reach the theoretical additive value.

Effect of H_2O_2 Dosages

To optimize the reaction conditions, the effect of initial H_2O_2 concentration on the degradation efficiency of aniline by Fe(VI) was investigated. The experiments were conducted with 10 mM aniline, 10 mM Fe(VI) at 30ºC. The results are presented in Fig. 2. The aniline removal efficiency exhibited a volcano-type trend, first increasing and then decreasing with the increasing H_2O_2 dosage. The removal efficiency significantly improved when the H_2O_2 concentration was raised from 10 mM to 176 mM. After 90 min of reaction, the aniline removal rate reached 98%. However, beyond this critical threshold of 176 mM, further increasing the H_2O_2 concentration introduced an inhibitory effect, resulting in a decline in removal efficiency.

This phenomenon can be explained by the dual role of H_2O_2 in the system. At low H_2O_2 concentrations, the dosage was insufficient to fully react with Fe(VI). The limited number of H_2O_2 molecules could neither effectively reduce Fe(VI) to generate adequate amounts of highly reactive iron species (Fe(IV)/Fe(V)) or free radicals (·OH), nor overcome the consumption by competing pathways, leading to constrained degradation efficiency [10, 23]. As the H_2O_2 concentration increased to 176 mM, the provided reducing capacity reached a more favorable stoichiometric ratio with Fe(VI). Sufficient H_2O_2 efficiently activates Fe(VI), promoting the continuous generation of reactive species such as Fe(IV)/Fe(V) and ·OH via pathways illustrated in Eqs. (1)-(4). Furthermore, Fe(III), a reduction product of Fe(VI), could be reduced to Fe(II) by H_2O_2 (Eq. 5), and the resultant Fe(II) subsequently catalyzed the production of additional ·OH via a Fenton-like reaction (Eq. 6). This established a synergistic catalytic cycle, significantly accelerating aniline degradation.

However, when H_2O_2 was excessively applied (>176 mM), its role as a scavenger became dominant. The surplus H_2O_2 participated in competitive side reactions with the reactive species, for instance, it reacted with ·OH to form HO_2·, which has a lower redox potential (Eq. 7); it promoted the self-quenching of ·OH (Eq. 8); and it might directly reduce and consume the highly reactive Fe(IV)/Fe(V) intermediates. These side reactions not only consumed H_2O_2 unproductively but, more critically, diminished the effective concentration of reactive species available for oxidizing aniline, thereby resulting in the observed decrease in macroscopic degradation efficiency [20].

$$Fe^{3+} + H_2O_2 \longrightarrow Fe^{2+} + HO^+ + HO_2 \cdot \quad (5)$$

$$Fe^{2+} + H_2O_2 \longrightarrow Fe^{3+} + HO^- + \cdot OH \quad (6)$$

$$H_2O_2 + \cdot OH \longrightarrow H_2O + HO_2 \quad (7)$$

$$\cdot OH + \cdot OH \longrightarrow H_2O_2 \quad (8)$$

Effect of Temperature

The influence of reaction temperature on the degradation of aniline by the Fe(VI)–H_2O_2 system was investigated under fixed conditions (10 mM aniline, 10 mM Fe(VI), 176 mM H_2O_2, pH = 7). The degradation behavior over the temperature range of 10-60ºC is shown in Figs 3 and 4. As the temperature increased

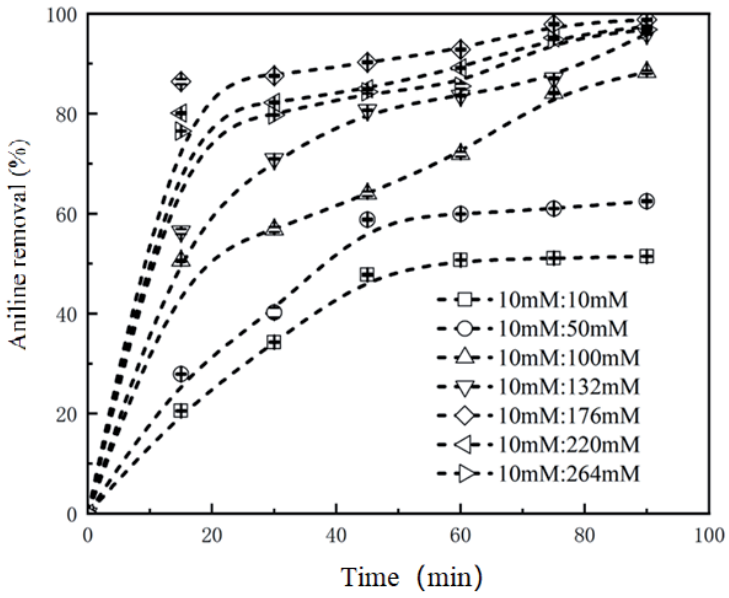

Fig. 2. Effect of H_2O_2 dosages on the degradation rate of aniline.
(Reaction conditions: T = 30ºC, pH = 7, 10 mM aniline, 10 mM Fe(VI)).

from 10ºC to 30ºC, the degradation efficiency of aniline markedly improved, and the apparent reaction rate constant (k_{app}) increased from 0.02057 min^{-1} to 0.07319 min^{-1}, indicating that elevated temperature enhanced the oxidative capacity of the Fe(VI)–H_2O_2 system. This trend is consistent with the report by Sun et al. [24]. The temperature rise not only accelerated the direct oxidation of aniline by Fe(VI) but also promoted the decomposition of Fe(VI) to form Fe(II)/Fe(III). These lower-valent iron species could further activate H_2O_2 [13], inducing Fenton-like reactions that continuously generate ·OH, thereby establishing an autocatalytic cycle and enhancing the synergistic effect between Fe(VI) and H_2O_2.

However, when the temperature was further increased from 30ºC to 60ºC, the removal efficiency of aniline decreased, with the k_{app} value dropping to 0.0298 min^{-1}, indicating an inhibitory effect at excessively high temperatures. High temperatures reduce the thermal stability of oxidants. The weak lattice energy of Fe(VI) led to accelerated auto-decomposition at high temperatures [25], causing the loss of effective species before they could participate in the target reaction. Simultaneously, H_2O_2 decomposed more rapidly at

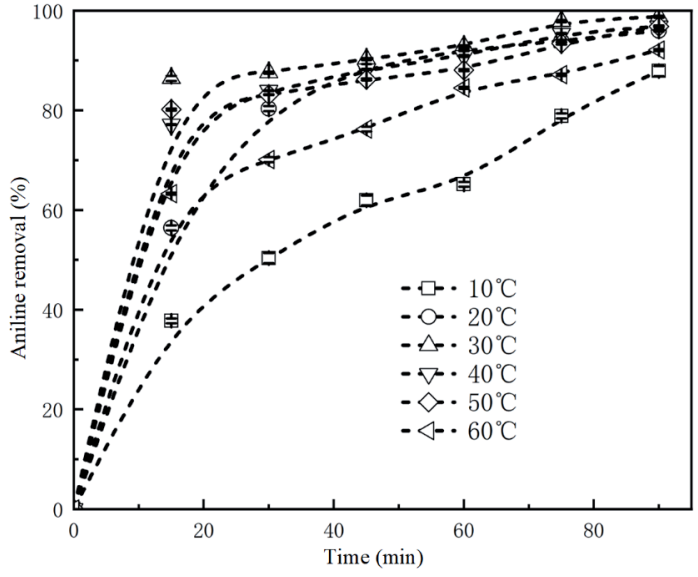

Fig. 3. Effect of temperature on the degradation of aniline.

elevated temperatures, compromising its sustainable supply. At high temperatures, enhanced scavenging of reactive species occurred, and the increased reactivity promoted the self-quenching of radical species such as ·OH [26], as well as their reaction with H_2O_2 to generate HO_2·, which has lower oxidative capacity [20], thereby reducing the concentration of effective oxidizing species. Byproducts and intermediates such as azobenzene were accumulated [8], and high temperatures may promote side reactions, leading to the formation of more stable and refractory intermediates or polymers that hinder further degradation. Although high temperature increased the initial reaction rate, it also caused rapid consumption of Fe(VI) and H_2O_2 within the first 45 min. The system reached a plateau prematurely, and the degradation stalled in the later stages due to insufficient oxidants.

In conclusion, temperature critically regulates the degradation performance of the Fe(VI)–H_2O_2 system by affecting oxidant stability, the balance between generation and consumption of radicals, and reaction pathways. Based on the degradation profiles in Fig. 4, 30ºC is identified as the suitable temperature for aniline degradation in this system.

Effect of pH

To elucidate the regulatory mechanism of pH on aniline degradation by the Fe(VI)-H_2O_2 system, experiments were conducted under fixed conditions (aniline: 10 mM; Fe(VI): 10 mM; H_2O_2: 176 mM; temperature: 30ºC) across a pH range of 3-11. The degradation behavior and kinetic profiles were investigated, as shown in Fig. 5 and Fig. 6. pH is a critical factor influencing the speciation, stability, and reaction pathways of Fe(VI). As illustrated in Fig. 6, Fe(VI) exists in different forms at varying pH levels, which directly dictates its redox potential and reactivity.

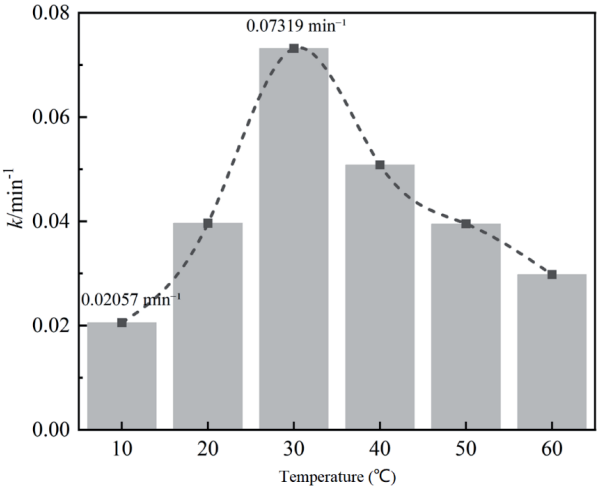

Fig. 4. Reaction rate constants (k) at different temperatures.

Under strongly acidic conditions (pH=3), Fe(VI) primarily exists as $H_3FeO_4^+$ and H_2FeO_4 [27], with a high standard redox potential ($E^o \approx +2.20$ V) [28], exhibiting strong direct oxidation capability. The removal rate of aniline reached 91±0.3% at 30 min; this was attributed to multiple synergistic effects: the decomposition of Fe(VI) in acidic medium generates Fe(III), which reacts with H_2O_2 in a Fenton-like process to continuously produce ·OH; meanwhile, ·OH possesses a higher oxidation potential (≈2.7 V) in acidic media [29]; increased solubility of Fe(II)/Fe(III) further promotes H_2O_2 decomposition and radical generation. Uncomplexed Fe(III) also accelerates Fe(VI) decomposition, forming a positive feedback loop. However, after 60 min, the removal efficiency slightly decreased compared to neutral conditions due to premature oxidant consumption. Kinetically, the process followed a pseudo-second-order model (k_{app} = 0.03425 $mM^{-1}\cdot min^{-1}$) (Fig. 6), suggesting a bimolecular reaction between Fe(VI) and aniline.

When pH increased to 5, the dominant Fe(VI) species shifted to $HFeO_4^-$ (Fig. 6), with a decreased redox potential (≈1.50 V) [30] and significantly reduced decomposition rate [31], weakening its direct oxidation capacity and leading to decreased aniline degradation efficiency.

At neutral pH (pH=7), the removal rate of aniline reached 88±0.2% at 30 min. Here, Fe(VI) exists as a mixture of FeO_4^{2-} and $HFeO_4^-$, with improved stability and diversified reaction pathways. Fe(VI) can attack water molecules, H_2O_2 [18], aniline [9], or generate highly reactive intermediates such as Fe(IV)/Fe(V) via self-decomposition (Eq. 9 to Eq. 12) [32]. The system contained multiple oxidative species, including Fe(IV)/Fe(V), ·OH, $O_2\cdot^-$, and aniline radicals, forming a complex synergistic degradation network. Consequently, the kinetics adhered to a pseudo-first-order model (k_{app} = 0.07319 min^{-1}).

$$Fe(VI) + H_2O \rightarrow Fe(IV) + H_2O_2 \quad (9)$$

$$Fe(VI) + H_2O_2 \rightarrow Fe(IV) + O_2\uparrow \quad (10)$$

$$Fe(VI) + aniline \rightarrow Fe(V) + aniline\cdot \quad (11)$$

$$Fe(VI) \rightarrow Fe(III) + O_2\uparrow + H_2O_2 \quad (12)$$

Under strongly alkaline conditions (pH = 11), the degradation rate decreased significantly (k_{app} = 0.02931 min^{-1}). At 30 min, the aniline removal efficiency was 59%, which is 32% lower than that achieved at pH 3. Fe(VI) became overly stable with reduced reactivity, and ·OH exhibited a lower redox potential (≈1.8 V). Fe(VI) predominantly underwent two-electron transfer reactions with H_2O_2 [33]; its decomposition product Fe(III) rapidly precipitated as $Fe(OH)_3$ (Eqs. 13 to 16), reducing interactions with H_2O_2; OH^- attacked H_2O_2, triggering futile decomposition (Eqs. 17 to 18). Additionally, aniline ($pK_a \approx 4.6$) [34]

exists predominantly in its free base form ($C_6H_5NH_2$) under strong alkalinity, and deprotonation renders it less susceptible to electrophilic attack [9], further impeding degradation (Eq. 19).

$$Fe(IV) + H_2O_2 \longrightarrow Fe(OH)_2 + O_2\uparrow \quad (13)$$

$$Fe(VI) + Fe(OH)2 \rightarrow Fe(V) + Fe(OH)_3 \quad (14)$$

$$Fe(V) + 4H_2O \rightarrow 2Fe(OH)_3 \downarrow + O_2 + 4OH^- \quad (15)$$

$$Fe(VI) + 2Fe(OH)_3 + 10OH- \rightarrow 3Fe(IV) + 5H_2O \quad (16)$$

$$OH^- + H_2O_2 \rightarrow HO_2 \cdot + H_2O \quad (17)$$

$$OH^- + H_2O_2 \rightarrow \cdot OH + \cdot O_2 - + H_2O \quad (18)$$

$$C_6H_5NH_3^+ + OH^- \rightleftharpoons C_6H_5NH_2 + H_2O \quad (19)$$

In summary, pH profoundly influences aniline degradation efficiency and kinetic models by modulating

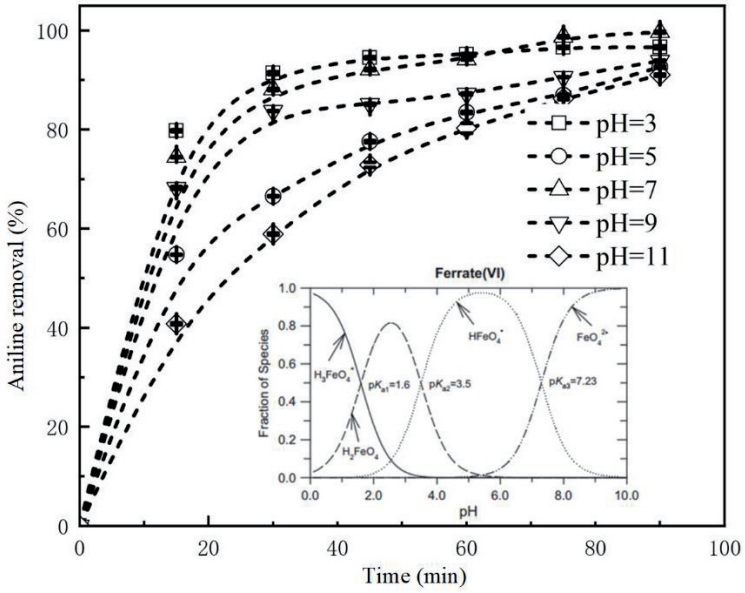

Fig. 5. Effect of pH on the degradation of aniline in Potassium Ferrate-Peroxide system.

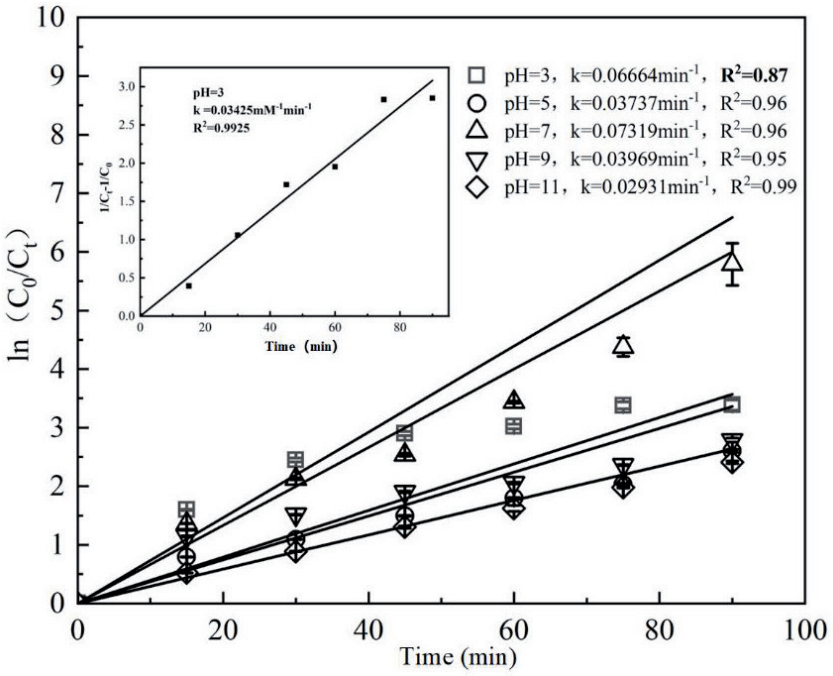

Fig. 6. Fitting diagrams of reaction kinetics at different pH values.

Fe(VI) speciation, stability, generation of reactive species, and reaction pathways. A stark contrast was observed between pH 3 and pH 11: after 30 min, the removal efficiency at pH 11 (59±0.3%) was 32±0.1% lower than that at pH 3, while the reaction kinetics transitioned from pseudo-second-order to pseudo-first-order, respectively. Under the investigated conditions, the system exhibited optimal degradation kinetics near neutral pH (pH = 7).

Free Radical Scavenging Experiment

To evaluate the contribution of free radicals to aniline degradation by the Fe(VI)-H_2O_2 system, radical quenching experiments were conducted. Following methods like those used by Li [9] and Fitri [35], tert-butanol (TBA) was selected as an effective scavenger for ·OH [36, 37]. The experiments were performed under conditions of T = 30ºC, 10 mM aniline, 10 mM Fe(VI) and 176 mM H_2O_2, in a 250 mL solution containing 100 mL TBA (creating a high-concentration scavenger environment). The degradation behavior of aniline at different pH levels was investigated, and the results are shown in Fig. 7(a-e).

The results indicate that the contribution of radicals is highly pH dependent. Under acidic conditions (pH = 3) (Fig. 7a)), the addition of TBA significantly reduced the aniline degradation rate from 96.5% to 45.2% at 45 min, a decrease of more than 50%. This strongly demonstrates that ·OH and other potentially inhibited radicals (e.g., $SO_4^{\cdot-}$) are the primary contributors to degradation at this pH, operating alongside the direct oxidation by Fe(VI). As pH increased, the proportional contribution of radicals gradually decreased. Under neutral conditions (pH=7) (Fig. 7c)), the degradation rate in the system with TBA was 62.9% at 15 min, significantly lower than the 80.9±0.2% observed in the system without the scavenger. This difference confirms that even in the neutral region, the radical pathway still contributes substantially (accounting for approximately 22% of the total degradation), indicating the coexistence of at least two parallel mechanisms in the Fe(VI)-H_2O_2 system under these conditions-namely, direct oxidation by Fe(VI) and/or high-valent iron species (Fe(IV)/Fe(V)), and ·OH-dominated radical oxidation.

Under alkaline conditions (pH≥9) (Fig. 7d) and e)), the degradation curves with and without TBA nearly overlapped, showing no significant difference. This indicates that the contribution of radicals becomes negligible. This finding aligns with reports in the literature [32, 38], suggesting a fundamental shift in the reaction pathway under alkaline environments; non-radical direct electron transfer becomes the dominant process. Here, Fe(VI) itself is more stable, and the intermediate iron species (Fe(IV)/Fe(V)) generated from its reduction possess higher reactivity than Fe(VI) [32], becoming the dominant agents degrading aniline. Besides potentially participating directly, H_2O_2 primarily acts to accelerate the reduction of Fe(VI), promoting the generation of highly reactive Fe(IV)/Fe(V) and thus indirectly enhancing degradation efficiency. The convergence of degradation rates after 60 min across systems suggests that different pathways can achieve similar endpoints given sufficient reaction time, although the kinetics and dominant mechanisms vary with pH.

These results demonstrate that pH not only regulates the speciation and stability of Fe(VI) but also profoundly influences the selection of reaction pathways in the Fe(VI)-H_2O_2 system: transitioning from radical-dominated processes under acidic conditions, to a synergy of radical and direct oxidation in the neutral region, and finally to a high-valent iron-mediated electron transfer mechanism under alkaline conditions.

Analysis of Products and Degradation Pathways

To further investigate the reaction mechanism of aniline degradation by the Fe(VI)-H_2O_2 system, liquid chromatography-mass spectrometry (LC-MS) was employed to analyze intermediate products formed during the process. A total of 14 major intermediates were identified (Fig. 8). The results indicate that the synergistic role of H_2O_2 not only involves promoting the generation of ·OH but, more critically, maintaining the oxidative cycle of highly reactive high-valent iron species such as Fe(IV)/Fe(V) through pathways including Eq. (20), thereby continuously driving the degradation process:

$$FeO_4^{4-} + H_2O_2 \rightarrow FeO_4^{2-} + H_2O + O_2 \quad (20)$$

The reaction pathways of the system exhibit strong pH dependence. Under acidic conditions, radical reactions (particularly involving ·OH) dominate the oxidation and polymerization processes. In contrast, under alkaline conditions, the stability of Fe(VI) increases, its self-decomposition is suppressed, and the reaction relies more on the direct oxidation capacity of high-valent iron species (Fe(IV)/Fe(V)) rather than ·OH-induced chain reactions. Sun et al. [24] identified key intermediates such as nitrobenzene, azobenzene, and p-benzoquinone using gas chromatography-mass spectrometry (GC-MS), which is highly consistent with the LC-MS results obtained in this study, further validating the proposed degradation pathways.

We propose that aniline degradation in the Fe(VI)-H_2O_2 system may proceed via the following four main pathways:

Path 1: ·OH attacks the benzene ring of aniline, leading to hydroxylation and the formation of hydroxyaniline (C_6H_5NHOH), which is further oxidized via deamination to hydroquinone ($C_6H_4(OH)_2$) and ultimately ring-opened to yield p-benzoquinone ($C_6H_4O_2$) and its derivatives.

Path 2: Fe(VI) oxidizes aniline via a single-electron transfer mechanism, generating an aniline radical cation ($C_6H_5NH_2$·) while being reduced to Fe(V). Fe(V) further participates in reactions through a two-electron transfer mechanism. ·OH or high-valent iron species attack the amino group, resulting in dehydrogenation and the formation of nitrosobenzene (C_6H_5NO), which is ultimately oxidized to nitrobenzene ($C_6H_5NO_2$) and hydroxynitrobenzene ($NO_2C_6H_4OH$) [24].

Path 3: Aniline radical intermediates ($C_6H_5NH^{\cdot}$) undergo coupling reactions to form azobenzene ($C_{12}H_{10}N_2$). The benzene rings are further subjected

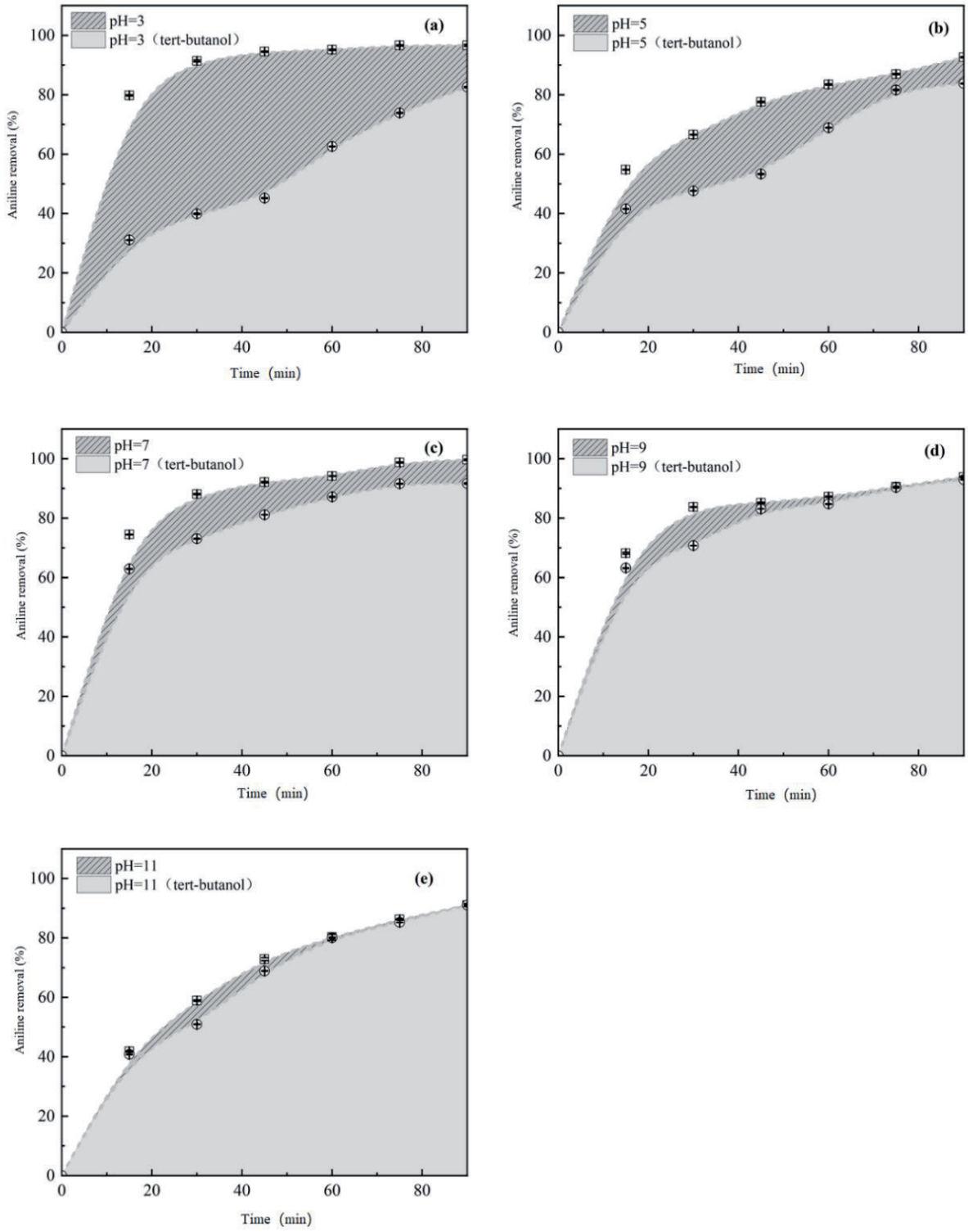

Fig. 7. Effect of the hydroxyl radical scavenger tert-butanol (TBA) on aniline degradation by the Fe(VI)/H_2O_2 system at different initial pH values. a) pH 3.0, b) pH 5.0, c) pH 7.0, d) pH 9.0, e) pH 11.0. (Reaction conditions: 10 mM aniline, 10 mM Fe(VI), 176 mM H_2O_2, 30ºC, with or without 100 mL TBA in a 250 mL reaction solution).

to electrophilic attack, leading to nitration and the formation of nitroazobenzene ($C_{12}H_9N_3O_2$), which eventually undergoes ring-opening reactions to yield small amide molecules such as succinamide ($NH_2COC_2H_4CONH_2$).

Path 4: Radical attack at the para-position of the benzene ring promotes dimerization, forming compounds such as 4-aminobiphenyl ($C_{12}H_{11}N$), which is further oxidized and ring-opened to generate small molecular aldehydes and carboxylic acids (e.g., glyoxylic acid ($C_2H_2O_3$) and formic acid (CH_2O_2)), ultimately mineralizing completely into CO_2 and H_2O.

In summary, the Fe(VI)-H_2O_2 system efficiently degrades aniline through multiple pathways, with the dominant route being regulated by pH. The final products tend to be small molecular acids and mineralized end products. The presence of intermediates shared with the Fe(VI)-only system [24] indicates that H_2O_2 enhances the intrinsic Fe(VI) pathways without altering their fundamental nature. Furthermore, while Fitri et al. [20] focused on pH 6-8, we found that more acidic conditions (e.g., pH 3) unlock a pronounced radical-mediated mechanism, leading to superior degradation efficiency. This distinct mechanistic shift under different pH regimes was definitively established through radical quenching experiments. Relevant prior studies were listed in Table 1.

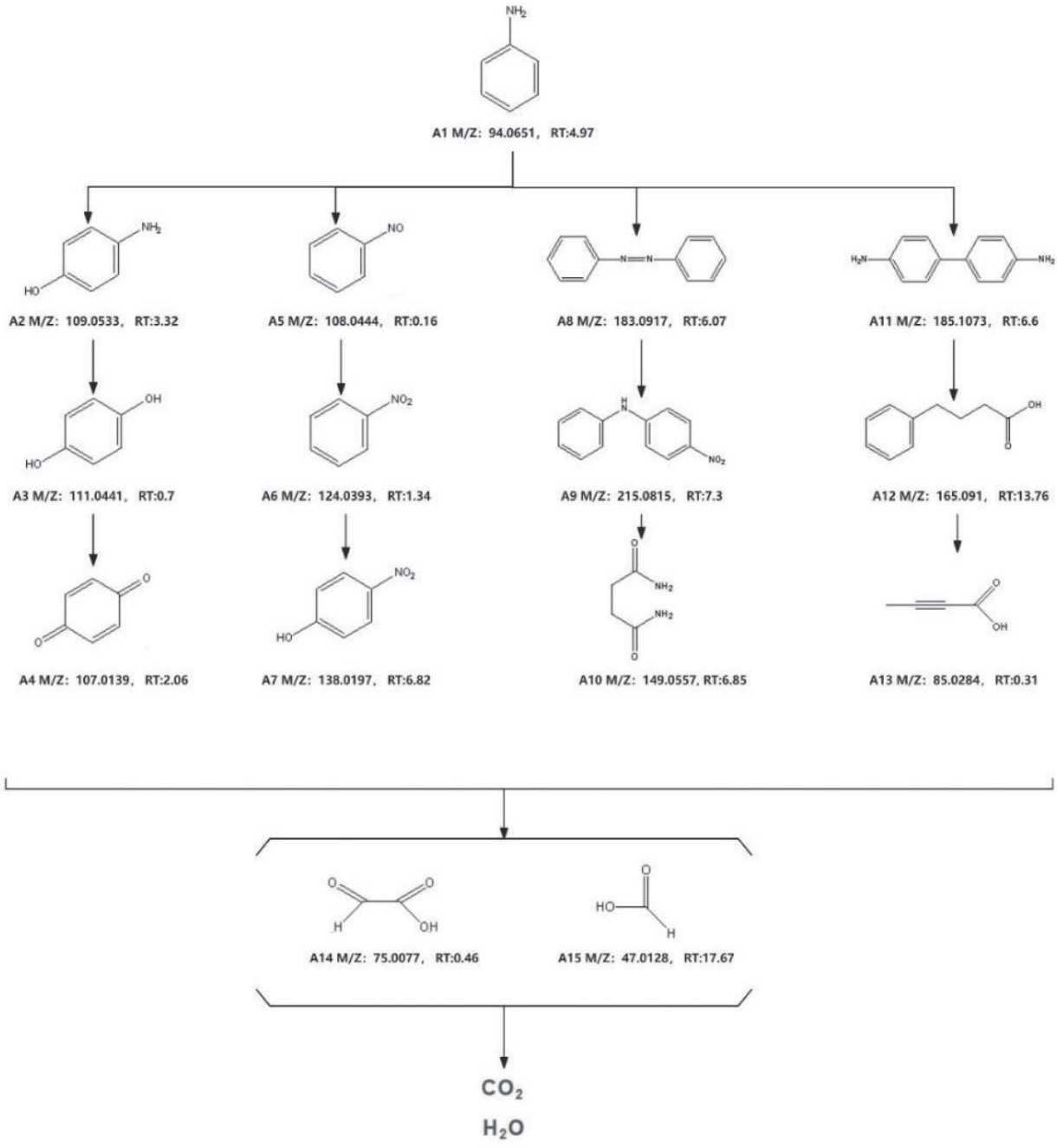

Fig. 8. Intermediate products of aniline degradation.

Table 1. Comparative study on the degradation of organic pollutants by Fe(VI) oxidation systems.

Oxidation system	Degraded Substances	Removal Rate	Experimental Conditions	Mechanism	Ref.
Fe(VI)	Aniline	--	pH = 6-10, T = 25℃ [Fe(VI)] = 50-100 μM, [Aniline]>10[Fe(VI)]	Free Radicals	[8]
Fe(VI)-H_2O_2	Sulfamethoxazole (SMX)	78%	pH = 7.0-9.0, t = 300 s, [Fe(VI)] = 100μM, [H_2O_2] = 770 μM	Free Radicals + Electron transfer	[10]
Fe(VI)-H_2O_2	Bisphenol A (BPA)	99.5%	pH = 8.0, t = 60 min, BPA = 50, 200 or 1,000 μg/L, [Fe(VI)]/[H_2O_2] = 1050 : 5000 or 250 : 2500	Free Radicals	[11, 20]
Fe(VI)-H_2O_2	Dimethyl Phthalate (DMP)	89.7%	pH = 7, t = 360 min, Fe(VI)]/[H_2O_2]/[DMP] = 10:2:1	Free Radicals	[13]
Fe(VI)-H_2O_2	Sulfamethoxazole (SMX)	70.81%	pH = 3, t = 90 min, SMX = 2 mg/L, [Fe(VI)]/[H_2O_2] = 1:5.5	Free Radicals	[14]
Fe(VI)-H_2O_2	Methyl Phenyl Sulfoxide (PMSO)	>80%	pH = 8.0 ± 0.2, [Fe(VI)] = 600 μM, [H_2O_2] = 1.2 mM, [PMSO] = 50 or 12 μM	Free Radicals +Electron transfer	[18]
Fe(VI)-H_2O_2	Chemical Oxygen Demand (COD)	68%	pH = 8.0, T = 25℃, Fe(VI) = 1500 mg/L, [H_2O_2] = 0.05 mol/L	Free Radicals	[39]
Fe(VI)-H_2O_2	Phenanthrene (PHE)	84.01%	pH = 5, t = 360 min, Fe(VI)]/[H_2O_2]/[PHE] = 2:2:1	--	[40]
Fe(VI)-$H_{2O}2$	Atrazine	15.9%	pH = 6.0, T = 25ºC, [H_2O_2] = 5.0 mM, [Fe(VI)] = 2.5 mM, [atrazine] = 46.5 μM	--	[41]
Fe(VI)-H_2O_2	Aniline	pH = 3.0, 91±0.3%. pH = 7.0, 88±0.2%	pH = 3-11, T = 10-60ºC, [Aniline] = 10 mM, [Fe(VI)] = 10 mM, [H_2O_2] = 10-176 mM, t = 30 min	Free Radicals +Electron transfer	Our works

Conclusions

This study investigated the oxidative degradation of aniline using the Fe(VI)/H_2O_2 system, revealing the degradation mechanisms and pathway evolution over a broad pH range (3-11). The results demonstrated that under the conditions of T = 30ºC, 10 mM aniline, 10 mM Fe(VI), and 176 mM H_2O_2, the reaction followed pseudo-first-order kinetics (k_{app} = 0.07319 min^{-1}), which was significantly higher than that observed in single-oxidant systems. Under acidic conditions (pH = 3), the Fe(VI)/H_2O_2 system exhibited second-order kinetics (k_{app} = 0.03425 $mM^{-1}\cdot min^{-1}$). Combined with radical quenching experiments, the regulatory role of pH on the reaction pathway was clarified: under acidic conditions, radicals (such as ·OH) served as one of the dominant oxidizing species, whereas under alkaline conditions, direct oxidation via electron transfer by Fe(VI) became predominant. LC-MS analysis identified 14 intermediate products, and four degradation pathways were proposed – hydroxylation, nitration, coupling, and ring-opening – elucidating the dual role of H_2O_2 dosage in both promoting and inhibiting Fe(VI) oxidation. Specifically, an appropriate concentration of H_2O_2 enhances the oxidative efficiency of Fe(VI), while an excess has an inhibitory effect. A major limitation of this study is the lack of investigation into the influence of common coexisting ions (e.g., Cl^-, HCO_3^-) in real water bodies on degradation efficiency. Future work should include validation studies using authentic water samples.

While the optimal conditions herein were derived from single-factor experiments, future work employing statistical experimental design (e.g., Response Surface Methodology) could further refine the operational parameters and elucidate factor interactions for specific wastewater applications.

Acknowledgments

This work was supported by the Science and Technology Program (LMTD202102) and the Innovation Team Program of Liming Vocational University (PCL20061).

Conflict of Interest

The authors declare no conflict of interest.

References

1. CHATURVEDI N.K., KATOCH S.S. Remedial technologies for aniline and aniline derivatives elimination from wastewater. Journal of Health Pollution, **10** (25), 1, **2020**.

2. WANG X., WANG Y., SHU Z., CAO Y., WANG X., ZHOU F, HUANG J. Phenolic hydroxyl-functionalized hyper-cross-linked polymers for efficient adsorptive removal of aniline. Separation and Purification Technology, **305**, 122443, **2023**.
3. O'NEILL F., BROMLEY-CHALLENOR K., GREENWOOD R., KNAPP J. Bacterial growth on aniline: implications for the biotreatment of industrial wastewater. Water Research, **34** (18), 4397, **2000**.
4. TANG Z., XU C., SHEN C., SUN S., MENG X., WANG S., L.I. Evaluation of Key Intermediates in Azo Dye Degradation by Advanced Oxidation Processes: Comparing Anilines and Phenols. ACS ES and T Water, **4** (11), 4872, **2024**.
5. MANNA M., SEN S. Advanced oxidation process: a sustainable technology for treating refractory organic compounds present in industrial wastewater. Environmental Science and Pollution Research, **30** (10), 25477, **2023**.
6. VELO-GALA I., LÓPEZ-PEÑALVER J.J., SÁNCHEZ-POLO M., RIVERA-UTRILLA J. Comparative study of oxidative degradation of sodium diatrizoate in aqueous solution by H_2O_2/Fe^{2+}, H_2O_2/Fe^{3+}, Fe(VI) and UV, H_2O_2/UV, $K_2S_2O_8$/UV. Chemical Engineering Journal, **241**, 504, **2014**.
7. SHARMA V.K., KAZAMA F., HU J., RAY A.K. Ferrates (iron(VI) and iron(V)): Environmentally friendly oxidants and disinfectants. Journal of Water Health, **3** (1), 45, **2005**.
8. SUN S., LIU Y., MA J., PANG S., HUANG Z., GAO Y., XUE M., YUAN Y., JIANG J. Transformation of substituted anilines by Ferrate (VI): Kinetics, pathways, and effect of dissolved organic matter. Chemical Engineering Journal, **332**, 245, **2018**.
9. GUO J., WANG S., LI T., WANG L., YOU H. A new perspective on contaminants as "activators": Aromatic amine groups promoted degradation of tetracycline by Ferrate (VI). Journal of Hazardous Materials, **479**, 135740, **2024**.
10. LUO M., ZHOU H., ZHOU P., LAI L., LIU W., AO Z., YAO G., ZHANG H., LAI B. Insights into the role of in-situ and ex-situ hydrogen peroxide for enhanced Ferrate (VI) towards oxidation of organic contaminants. Water Research, **203**, 117548, **2021**.
11. WIDHIASTUTI F., FAN L., PAZ-FERREIRO J., CHIANG K. Oxidative treatment of bisphenol A by Fe(VI) and Fe(VI)/H_2O_2 and identification of the degradation products. Environmental Technology Innovation, **28**, 102643, **2022**.
12. LUO C., FENG M., SHARMA V.K., HUANG C.H. Revelation of Ferrate (VI) unimolecular decay under alkaline conditions: Investigation of involvement of Fe(IV) and Fe(V) species. Chemical Engineering Journal, **388**, 124134, **2020**.
13. XUE J., ZHU Z., ZONG Y., HUANG C., WANG M. Oxidative Degradation of Dimethyl Phthalate (DMP) by the Fe(VI)/H_2O_2 Process. ACS Omega, **4** (5), 9467, **2019**.
14. SHEIKHI S., JEBALBAREZI B., DEHGHANZADEH R., MARYAMABADI A., ASLANI H. Sulfamethoxazole oxidation in secondary treated effluent using Fe(VI)/PMS and Fe(VI)/H_2O_2processes: Experimental parameters, transformation products, reaction pathways and toxicity evaluation. Journal of Environmental Chemical Engineering, **10** (3), 107446, **2022**.
15. SHI W., LI M., ZHANG P., QIAN C., LIANG Z. Two-stage synergistic oxidation treatment of neomycin sulfate wastewater by potassium ferrate and hydrogen peroxide. Desalination Water Treat, **238**, 260, **2021**.
16. LACINA P., GOOLD S. Use of the ferrates (Fe IV–VI) in combination with hydrogen peroxide for rapid and effective remediation of water–laboratory and pilot study. Water Science and Technology, **72** (10), 1869, **2015**.
17. SHARMA V.K., GRAHAM N.J.D., LI X.Z., YUAN B.L. Ferrate(VI) enhanced photocatalytic oxidation of pollutants in aqueous TiO_2 suspensions. Environmental Science and Pollution Research, **17** (2), 453, **2010**.
18. WEN K., ZHANG Y., XU J., WANG X., ZHENG T., YANG Z., ZHENG G., HUANG Y., ZHANG J. New insights into magnetic fields selective enhancement of ferrate(VI) combined with hydrogen peroxide for removal of organic pollutants. Separation and Purification Technology, **351**, 128087, **2024**.
19. China Standards Press. Water Quality Determination of Aniline Compounds N-(1-Naphthyl) Ethylenediamine Azobenzene Spectrophotometric Method: GB/T 11889-1989. **1989**.
20. WIDHIASTUTI F., FAN L., PAZ-FERREIRO J., CHIANG K. Oxidative degradation of bisphenol A in municipal wastewater reverse osmosis concentrate (ROC) using Ferrate(VI)/hydrogen peroxide. Process Safety and Environmental Protection, **163**, 58, **2022**.
21. DAR A.A., PAN B., QIN J., ZHU Q., LICHTFOUSE E., USMAN M., WANG C. Sustainable ferrate oxidation: Reaction chemistry, mechanisms and removal of pollutants in wastewater. Environmental Pollution, **290**, 117957, **2021**.
22. WIDHIASTUTI F., FAN L., PAZ-FERREIRO J., CHIANG K. Oxidative treatment of bisphenol A by Fe(VI) and Fe(VI)/H_2O_2 and identification of the degradation products. Environmental Technology & Innovation, **28**, 102643, **2022**.
23. JUNJIE W.U., TINGMEI W., JIAYING P., XIAOXIA L., ZHONG W., LIQI W. Degradation Effect of Potassium Ferrate Combined with Hydrogen Peroxide on Florfenicol in Water. Animal Husbandry and Feed Science, **45** (4), 41, **2024**.
24. JUNG S.Y., KIM I.K. Degradation of aniline by liquid Ferrate(VI). Desalination and Water Treatment, **136**, 245, **2018**.
25. ZHANG X.Y., YANG C.C., GAO J. Preparation and Crystal Structure of K_2FeO_4. Chinese Journal of Synthetic Chemistry, **13** (4), 391, **2005** [In Chinese].
26. WANG T., XIE Y., LENH P.D., LE T., ZHANG L. Lead Recovery from Flue Dust by Using Ultrasonic-Enhanced Hydrogen Peroxide Water Washing. Recycling, **10** (4), 150, **2025**.
27. SHARMA V.K. Potassium Ferrate (VI): an environmentally friendly oxidant. Advances in Environmental Research, **6** (2), 143, **2002**.
28. CAO J.Y., DU Y., DAI X., LIU T., WANG Z., LI J., ZHANG H., ZHOU P., LAI B. Ferrate (VI)-based synergistic oxidation processes (Fe(VI)-SOPs): Promoted reactive species production, micropollutant/microorganism elimination, and toxicity reduction. Chemical Engineering Journal, **489**, 151180, **2024**.
29. RUSH J.D., ZHAO Z., BIELSKI B.H.J. Reaction of Ferrate (VI)/Ferrate (V) with Hydrogen Peroxide and Superoxide Anion - a Stopped-Flow and Premix Pulse Radiolysis Study. Free Radical Research, **24** (3), 187, **1996**.
30. SHARMA V.K. Ferrate (VI) and ferrate(V) oxidation of organic compounds: Kinetics and mechanism. Coordination Chemistry Reviews, **257** (2), 495, **2013**.

31. XIE X.F. Degradation of Aniline in Wastewater with Sulfate Radical Advanced Oxidation Technology Based on Activated Persulfate. Thesis, South China University of Technology, **2012** [In Chinese].
32. ZHU J., YU F., MENG J., SHAO B., DONG H., CHU W., CAO T., WEI G., WANG H., GUAN X. Overlooked Role of Fe(IV) and Fe(V) in Organic Contaminant Oxidation by Fe(VI). Environmental Science& Technology, **54** (15), 9702, **2020**.
33. DING C.S., XIAO M.H., ZHAO S.D., MIAO S.M., ZOU S.N. Performance of 2,6-DCBQ degradation in drinking water by potassium ferrate. Journal of Zhejiang University of Technology, **46** (3),337, **2018** [In Chinese].
34. LUKEŠ V., HARTMANN H. On the NH and CH acidities of toluidine isomers: theoretical description and practical consequences for the synthesis of certain aniline dyes. Coloration Technology, **137** (4), 389, **2021**.
35. WIDHIASTUTI F., FAN L., PAZ-FERREIRO J., CHIANG K. Oxidative treatment of bisphenol A in municipal wastewater reverse osmosis concentrate using Ferrate (VI). Journal of Environmental Chemical Engineering, **9** (4), 105462, **2021**.
36. WANG J., LI Y., YANG J., FENG Z., JING K., GUO K., ZHANG G. Oxidation of selected fluoroquinolones by Ferrate (VI) in water: Kinetics, mechanism, effects of constituents, and reaction pathways. Environmental Research, **243**, 117845, **2024**.
37. LEE Y., KISSNER R., VON GUNTEN U. Reaction of ferrate (VI) with ABTS and self-decay of ferrate (VI): kinetics and mechanisms. Environmental Science& Technology, **48** (9), 5154, **2014**.
38. LI G., JIANG J., HE M., RAO D., ZHANG J., SUN B. Enhancing Ferrate Oxidation of Micropollutants via Inducing Fe(V)/Fe(IV)Formation Needs Caution: Increased Conversion of Bromide to Bromate. Environmental Science and Technology, **57** (47), 18991, **2023**.
39. WENSHI L., YU L, YING X., XIAO X., CHUNYAN L., BO Y., XUNCHI P. Performances and mechanisms of Ferrate(VI) oxidation process for shale gas flowback water treatment. Process Safety and Environmental Protection, **173**, 120, **2023**.
40. LI Y.N., DUAN Z.H., WANG Y.F., YUAN Z.J., WAND G.Y. Preliminary treatment of phenanthrene in coking wastewater by a combined potassium ferrate and Fenton process. International Journal of Environmental Science and Technology, **16** (8), 4483, **2019**.
41. SHAOHUA W., HUIRU L., XIANG L., HUIJUN H., CHUNPING Y. Performances and mechanisms of efficient degradation of atrazine using peroxymonosulfate and ferrate as oxidants. Chemical Engineering Journal, **353**, 533, **2018**.